Supplementary Material (ESI) for Journal of Materials Chemistry

Electronic Supplementary Information for

Layer-by-layer assembly of layered double hydroxide/cobalt phthalocyanine ultrathin film and its application for sensors

Jingbin Han, Xiangyu Xu, Xiuying Rao, Min Wei,* David G. Evans and Xue Duan

State Key Laboratory of Chemical Resource Engineering, Beijing University of Chemical Technology, Beijing 100029, P. R. China.

CORRESPONDING AUTHOR FOOTNOTE

* Corresponding author. Phone: +86-10-64412131. Fax: +86-10-64425385. E-mail: weimin@mail.buct.edu.cn.

Figure S1 shows the XRD patterns of the MgAl-CO_3 and MgAl-NO_3 LDH samples, all of which can be indexed as a rhombohedral structure. The d_{003} basal spacing shifted from 7.58 Å (MgAl-CO_3 LDH) to 8.98 Å (MgAl-NO_3 LDH) after salt-acid treatment. No other crystalline phase was detected, indicating the high purity of the product. The results unambiguously indicate a complete replacement of interlayer CO_3^{2-} by NO_3^-. The SEM image of MgAl-NO_3 LDH (Figure S2) reveals mono-dispersive hexagonal crystals with a mean lateral dimension of 2~4 μm. The AFM image (Figure S3) displays a thin layer of morphologically irregular LDH nanosheet with lateral size of 2~4 μm, close to that of the MgAl-NO_3 LDH precursor. The average thickness of LDH nanosheets was *ca*. 0.8 nm, which was consistent with previous observations reported elsewhere.[1]

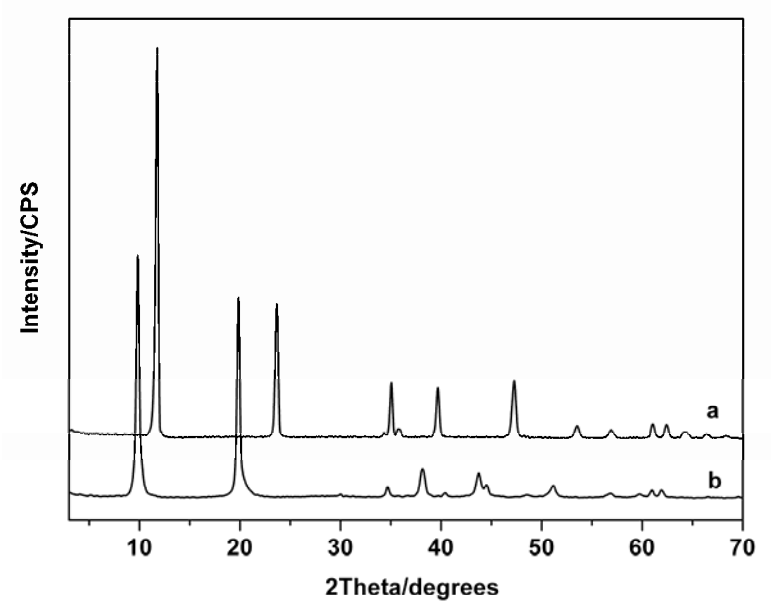

Figure S1. Powder XRD patterns of the (a) MgAl-CO_3 and (b) MgAl-NO_3 LDH samples (from our previous work ref. 2).

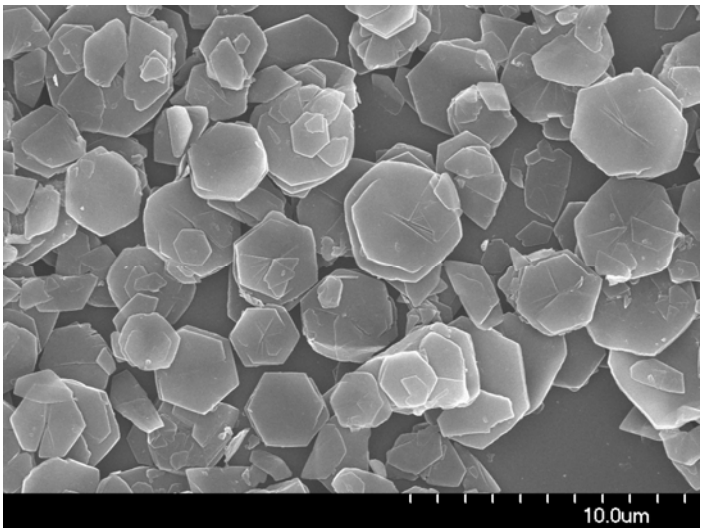

Figure S2. SEM image of the MgAl-NO_3 LDH precursor (from our previous work ref. 2).

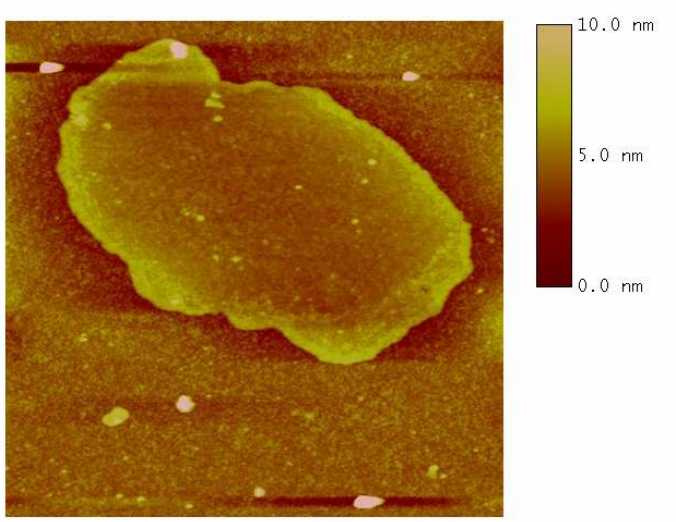

Figure S3. Tapping-mode AFM image for the exfoliated MgAl-LDH nanosheets deposited on a Si wafer substrate (bar scale: 4.0×4.0 μm) (from our previous work ref. 2).

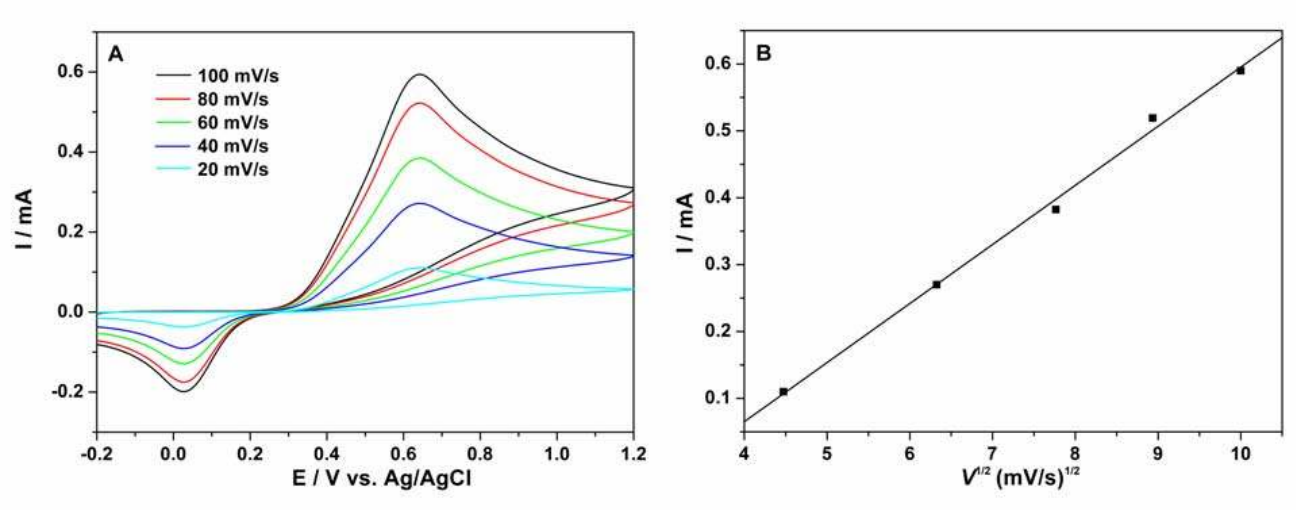

Figure S4. (A) Cyclic voltammograms of the $(LDH/CoPcTs)_6$ film in 0.1 mol/L PBS (pH 7.4) with the presence of 1×10^{-3} mol/L DA at various scan rates (20, 40, 60, 80, 100mV/s); (B) the linear relationship between the anodic peak current and the square root of scan rate.

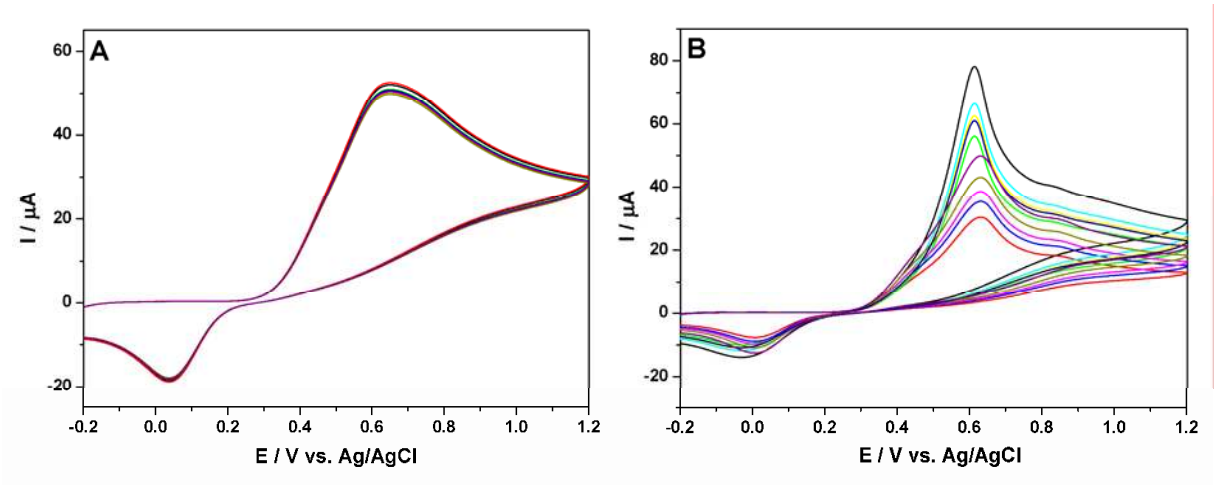

Figure S5. The measurement stability of (A) $(LDH/CoPcTs)_4$ and (B) $(PDDA/CoPcTs)_4$ modified electrode by recording cyclic voltammograms curves in 1.0×10^{-4} mol/L DA for 10 times (PBS 7.4, 100 mV/s).

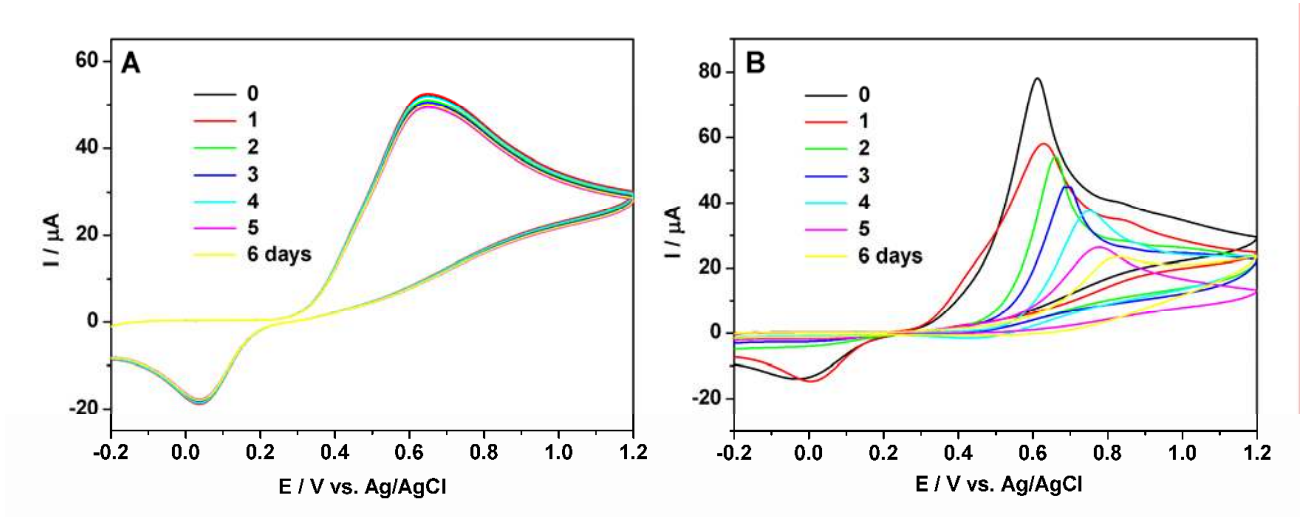

Figure S6. The long-term stability of (A) $(LDH/CoPcTs)_4$ and (B) $(PDDA/CoPcTs)_4$ modified electrode by recording cyclic voltammograms curves in 1.0×10^{-4} mol/L DA for consecutive 6 days (PBS 7.4, 100 mV/s).

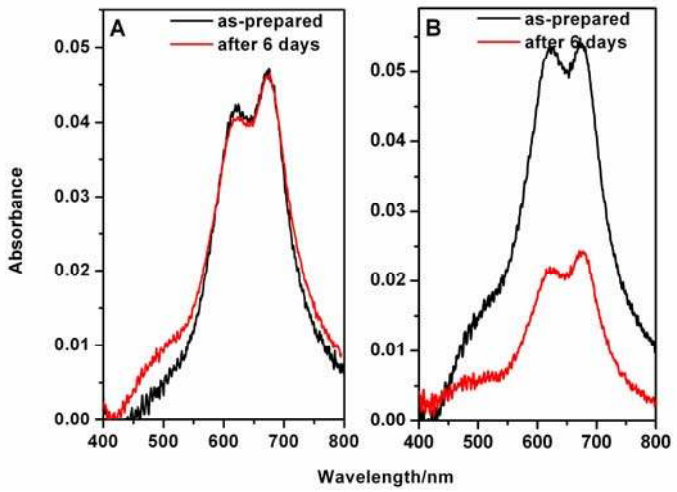

Figure S7. UV-vis absorption spectra of (A) $(LDH/CoPcTs)_4$ and (B) $(PDDA/CoPcTs)_4$ film before and after dipping into PBS (pH 7.4) for 6 days.

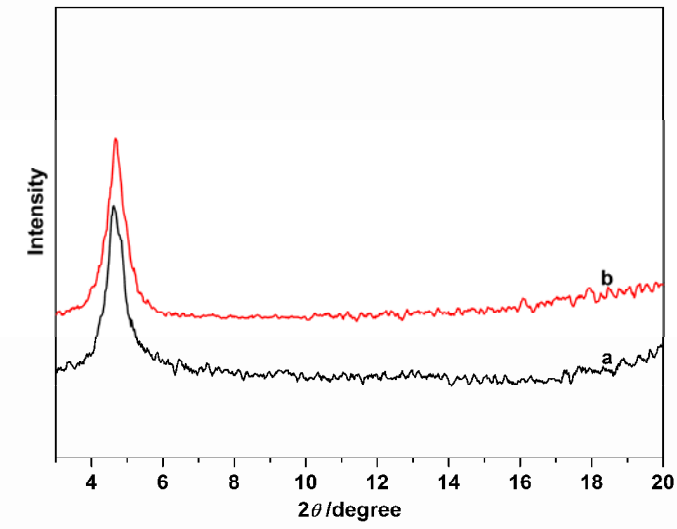

Figure S8. XRD patterns of $(LDH/CoPcTs)_4$ film before (a) and after dipping into PBS (pH 7.4) for 6 days (b).

References

1 (a) Z. P. Liu, R. Z. Ma, Y. Ebina, N. Iyi, K. Takada and T. Sasaki, *Langmuir*, 2007, **23**, 861; (b) Z. P. Liu, R. Z. Ma, M. Osada, N. Iyi, Y. Ebina, K. Takada and T. Sasaki, *J. Am. Chem. Soc*., 2006, **128**, 4872; (c) L. Li, R. Z. Ma, Y. Ebina, K. Fukuda, K. Takada and T. Sasaki, *J. Am. Chem. Soc*., 2007, **129**, 8000.

2 J. Han, J. Lu, M. Wei, Z. L. Wang and X. Duan, *Chem. Commun.*, 2008, 5188.